RESEARCH

Evaluation of organ dose using size-specific dose estimation (SSDE) and related cancer risk due to chest CT scan during the COVID-19 pandemic

Mostafa Robatjazi[1,2] · Mahdis Moayed[1] · Hamid Reza Baghani[3] · Mikaeil Molazadeh[4] · Nematullah Shomoossi[5]

Abstract

This study aimed to estimate lung and breast doses for individual patients using the size-specific dose estimate (SSDE) method, as well as calculating effective doses, in patients who underwent chest CT scans during the COVID-19 pandemic. Cancer risk incidence was estimated using excess relative risk (ERR), excess absolute risk (EAR), and lifetime attributable risk (LAR) models from the Biological Effects of Ionizing Radiation Report VII (BEIR-VII). Data from about 570 patients who underwent CT scans for COVID-19 screening were utilized for this study. Using the header of the CT images in a Python script, SSDE and effective dose were calculated for each patient. The SSDE obtained by water equivalent effective diameter (wSSDE) was considered as lung and breast dose, and applied in organ-specific cancer risk estimation. The mean wSSDE value for females (13.3 mGy) was slightly higher than that for males (13.1 mGy), but the difference was not statistically significant (P value = 0.41). No significant differences were observed between males and females in terms of calculated EAR and ERR for lung cancer at 5 and 30 years after exposure (P value = 0.47, 0.46, respectively). Similarly, there was no significant difference in lung cancer LAR values between females and males (P value = 0.48). The results also indicated a decrease in LAR values for both lung and breast cancers with increasing exposure age. In accordance with the ALARA (as low as reasonably achievable) principle, it is important for medical staff and the general public to consider the benefits of CT imaging in detecting such infections. Additionally, imaging medical physicists and CT scan experts should optimize imaging protocols and strike a balance between image quality for detecting abnormalities and radiation dose, all while adhering to the ALARA principle.

Keywords CT scan · SSDE · Organ dose · Effective dose · Cancer risk · COVID-19

Introduction

It has been approximately four years since the novel coronavirus SARS-CoV-2 (Severe Acute Respiratory Syndrome Coronavirus 2), commonly known as COVID-19, has emerged, which continues to affect human's life due to an acute respiratory infectious disease leading to death in some people (Hoda and Arash 2020; Vahdat et al. 2020). Typically, COVID-19 patients were reported to have experienced some symptoms such as dry cough, fever, fatigue, and sore throat. The reverse transcription enzyme chain reaction (RT-PCR) method using respiratory tract secretion specimens has been considered a gold standard reference for the diagnosis of COVID-19 infection, because of its sensitivity of more than 80% as reported in various studies (Williams et al. 2020).

✉ Hamid Reza Baghani
   Hamidreza.baghani@gmail.com

1. Department of Medical Physics and Radiological Sciences, Sabzevar University of Medical Sciences, Sabzevar, Iran

2. Non-Communicable Disease Research Center, Sabzevar University of Medical Sciences, Sabzevar, Iran

3. Department of Physics, Hakim Sabzevari University, Sabzevar, Iran

4. Department of Medical Physics, Tabriz University of Medical Sciences, Tabriz, Iran

5. School of Medicine, Sabzevar University of Medical Sciences, Sabzevar, Iran

As an alternative method for the detection of COVID-19 infection, chest computed tomography (CT) scans have been utilized. CT scans are well known for their ability to identify abnormalities such as multiple ground-glass opacities, patchy pulmonary consolidations, and crazy-paving patterns in the lungs of COVID-19 patients. In addition to their availability, ease of use, and quick scanning process, CT scans have demonstrated efficacy in assessing disease severity. The sensitivity of this method has been reported to reach up to 87%, indicating its capability to correctly identify positive cases. However, it is important to note that the specificity of CT scans for COVID-19 detection amounts to 46%, which highlights the potential for false-positive results (Khatami et al. 2020).

To this end, the utilization of CT scans for the early detection and assessment of COVID-19 disease severity has gained widespread adoption worldwide. However, the significant demand for this diagnostic method has raised concerns regarding the potential radiological consequences for patients. Consequently, low-dose protocols for chest CT scans in suspected COVID-19 patients have been proposed to mitigate radiation exposure (Kang et al. 2020; IAEA 2020; Homayounieh et al. 2020).

Some dose indexes in CT scanners such as volumetric CT dose index ($CTDI_{vol}$) and dose length product (DLP) have been employed to assess individual scan protocols both before and after the scanning procedures. The scan parameters, such as tube voltage, tube current, gantry rotation time, and pitch, do influence the values of CTDIvol and DLP. However, the dose received by a patient during a CT scan procedure depends on both the patient's body size and the scanner's radiation output. It is noted that the $CTDI_{vol}$ provides information solely about the scanner output. In fact, the $CTDI_{vol}$ is related to absorbed dose in two different dedicated phantoms (with a small diameter = 16 cm which is representative of the head, and a large diameter = 32 cm which is related to the body), and does not consider individual patient size effect in dose (Li et al. 2011). In a report of the Task Group (TG) 204 of the American Association of Physicists in Medicine (AAPM) the size-specific dose estimation (SSDE) approach has been introduced. SSDE is a dose estimation method that combines the physical dimensions of a patient, specifically the effective diameter, with the scanner output ($CTDI_{vol}$) to provide an estimate of the patient's radiation dose (Boone et al. 2011). To apply the SSDE approach, some conversion factors (reported in AAPM Report 204) were derived from experimental and Monte Carlo data and normalized to patient size in terms of water or tissue-equivalent materials. In this way, the geometric size of the body was considered as a surrogate of photon attenuation, which in turn is a physical phenomenon that can directly affect the absorbed dose. To address this concern, the report of TG 220 of AAPM has introduced the concept of water equivalent diameter (WED) which was derived from Hounsfield Units (HU) of CT images. This concept provides a more accurate representation of the attenuation properties of a patient's body tissues and has been used for SSDE (McCollough et al. 2014; Report 87 2012). There are some approaches for organ dose estimation in CT scans including the convolution method, Monte Carlo calculation, and the SSDE method. Among these methods, the SSDE approach is considered the easiest and most straightforward for this purpose. The use of SSDE for organ dose estimation has been investigated in various studies (Moore et al. 2014; Franck et al. 2016; Hardy et al. 2021). It is important to note that a necessary condition for organ dose estimation using SSDE is ensuring that the organ of interest is covered within the scan volume (Andersson et al. 2019; Moore et al. 2014). By considering the size-specific dose estimation and ensuring appropriate coverage of organs, the SSDE method offers a practical and accessible approach for estimating organ doses in CT scans, providing valuable insights for radiation dose management and optimization in clinical practice.

The objective of this study was to estimate the lung and breast doses for individual patients using the SSDE method, as well as calculate the effective dose for patients who underwent chest CT scans during the COVID-19 pandemic. Given the necessity of balancing the benefits of early pneumonia detection following COVID-19 infection with the potential risks of radiation-induced malignancy, the study also aimed to evaluate the risk of breast and lung cancer incidence in patients who underwent chest CT scans for COVID-19 screening. To assess the potential risks, the study utilized the National Research Council Biologic Effects of Ionizing Radiation (BEIR) VII models (NRC 2006).

Materials and methods

Patients and scanning devices

This retrospective study was conducted in accordance with an institutional ethically approved standard (IR.MEDSAB.REC.1400.151).

CT scan information of 570 COVID-19 patients admitted to three university hospitals was used in the present study. The data collection period spanned from July 2021 to September 2021. During this time period, data on CT scans performed for COVID-19 screening purposes were collected. Specific criteria were applied to ensure the relevance and accuracy of the data. The inclusion criteria encompassed patients who underwent chest CT scans for suspected or confirmed COVID-19 cases. Both adult and pediatric patients were included in the study. On the other hand, patients with incomplete or inadequate data were excluded from the analysis.

In the study, two of the hospitals utilized a Siemens Somatom Emotion 16 scanner, while the third hospital used a Toshiba Alexion 16 slice scanner. It is worth noting that even though the CT scanners in two of the hospitals were of the same model, the scanning protocols were optimized independently by different CT scan experts at each hospital. The optimization of scanning protocols involved adjustment of various parameters such as tube voltage, tube current, gantry rotation time, pitch, and choice of reconstruction algorithms, to achieve the desired image quality while minimizing radiation dose. It is also noted that different experts may have varying preferences, clinical requirements, or institutional guidelines, which can lead to variations in the scanning protocols, even with the same scanner model. These differences in scanning protocols can impact the radiation doses received by patients during CT scans. Optimal scanning protocols strike a balance between obtaining diagnostically useful images and keeping the radiation dose as low as reasonably achievable.

Because the study involved multiple hospitals with different CT scanner models and varying scanning protocols, it provides an opportunity to evaluate the impact of these factors on the radiation doses delivered to patients and their potential implications in terms of radiation risks and dose optimization strategies.

Dose values and SSDE methods

To obtain all dose information including $CTDI_{vol}$ and DLP, and to calculate SSDE and effective dose from the CT images, a Python code was prepared using different libraries to obtain information from CT images in digital imaging and communications in medicine (DICOM) format. The $CTDI_{vol}$, DLP, pixel size, and CT number of each pixel included in the header of the images, were used to calculate the SSDE and effective dose values by the use of this Python code.

Size-specific dose estimation

The SSDE values for each patient were calculated using the method described in the report of TG-204 by AAPM. This involved applying a conversion factor to calculate the SSDE from the $CTDI_{vol}$, taking into account the effective diameter (Eq. 1).

$$\text{SSDE} = f \times \text{CTDI}_{\text{vol}}. \tag{1}$$

The initial step involved obtaining the effective diameter from the CT images, which serves as a surrogate for the diameter of a circular shape in cases where the body shape is elliptical. To accomplish this, the anterior–posterior (AP) and lateral (Lat) diameters were utilized as in Eq. 2:

$$\text{Effective diameter} = \sqrt{\text{AP} \times \text{Lat}}. \tag{2}$$

To obtain the AP and LAT diameters from the images, the number of pixels in each direction (AP and LAT) was multiplied by the corresponding pixel dimension. This calculation provided the geometric diameter (GD) of the region of interest.

However, to account for the WED in the SSDE calculation, the method proposed by TG-220 of AAPM (McCollough et al. 2014) was followed. The primary focus of this method is the CT number calculation, which involves normalizing the CT numbers to the water attenuation coefficient (Eq. 3):

$$A_{\text{water}} = \sum \left(\frac{CT\#}{1000} + 1 \right)^{\alpha} \times A_{\text{pixel}}, \tag{3}$$

where the A_{water} is the water equivalent size of any pixel in the images, CT# represents the Hounsfield Unit (HU) of each pixel, α shows the weight of linear attenuation coefficients relative to water which has been assumed to equal one ($\alpha = 1$) based on previous studies (Ravenel et al. 2001; Toth et al. 2007; Menke 2005; Moore et al. 2014), and A_{pixel} represents the pixel size.

The pixel dimensions in the CT images are equal in each direction, forming a square shape. Given this characteristic, it is possible to extract one dimension of the pixel size from the DICOM header of the images. By summing these values in the AP and LAT directions, the body diameter can be calculated in each of these directions. Subsequently, Eq. (2) was employed to calculate the effective diameter.

In the first step of the WED calculation, the Python code calculated the water equivalent value for each individual pixel. The one-dimensional size of the pixels was then extracted. The WED value was obtained by summing up these values in the AP and LAT directions. Finally, the effective WED was determined using Eq. (2).

Figure 1 illustrates the calculation process for both the geometric and water equivalent effective diameters, providing visual representation of the steps involved in determining these parameters.

After calculation of effective diameters (geometric and water equivalent), the conversion factor (*f*) introduced in Eq. (1) was automatically calculated in the Python code using Eq. (4), which was introduced in an appendix of the AAPM TG-204 report (Boone et al. 2011) as Eq. A-1.

$$f = 3.704369 \times e^{-0.03671937 \times \text{effective diameter}}. \tag{4}$$

Due to the consideration of two different effective diameters (WED and GD), it was necessary to calculate their respective *f* values separately and, consequently, obtain two different values of SSDE. The SSDE values associated with the application of WED in the calculation of the *f*
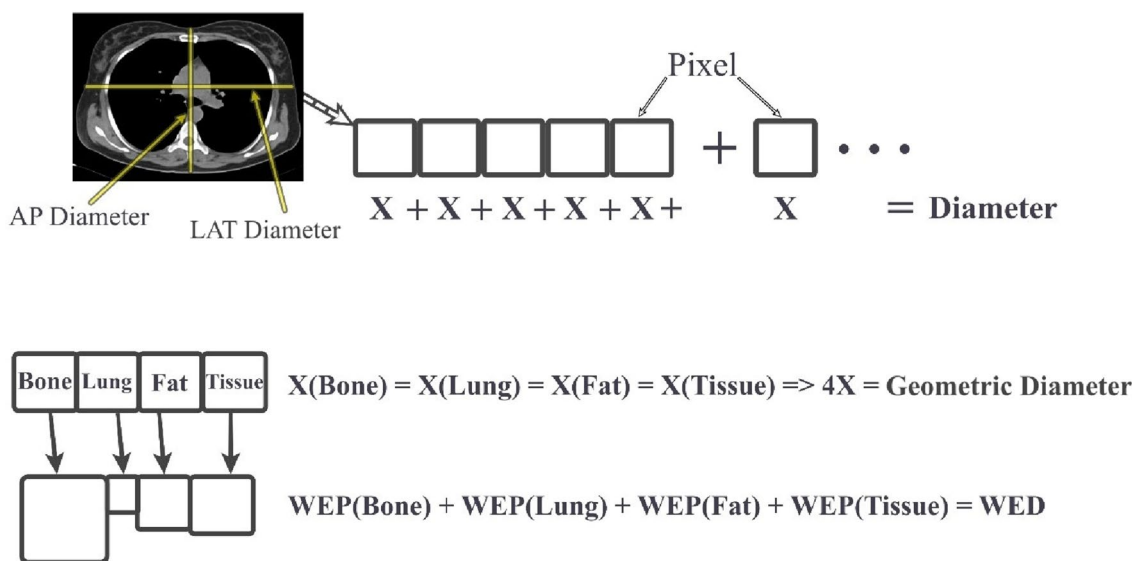
Fig. 1 The process of calculating the geometrical and water equivalent effective diameter (WED) from CT images. WEP stands for water equivalent pixel size for various tissues in CT images. *AP* anterior–posterior, *LAT* lateral

value will here be referred to as wSSDE (water equivalent SSDE), while the gSSDE (geometric SSDE) is related to the utilization of GD for the calculation of the *f* value.

Having both wSSDE and gSSDE allows for a comprehensive assessment of size-specific dose estimates considering different aspects of the patient's anatomy and tissue density. This dual approach provides a comprehensive understanding of the radiation dose received during CT imaging and facilitates an accurate evaluation of the potential risks associated with the procedure.

Effective dose

To calculate the effective dose, a conversion factor (k) multiplied by the DLP values was extracted from the Radiation Dose Structured Report (RDSR) of each patient (Eq. 5).

$$\text{Effecitve Dose(mSv)} = \text{Conversion factor}(k) \times \text{DLP}. \quad (5)$$

The conversion factor used in the present study was introduced by McCollough et al. (2008). The introduced conversion factors are specific to different anatomical regions and provide a relationship between the DLP and the effective dose in terms of mSv per mGy per centimeter ($\text{mSv.mGy}^{-1}.\text{cm}^{-1}$). In the case of chest for adults, the conversion factor was reported as 0.014 $\text{mSv.mGy}^{-1}.\text{cm}^{-1}$ which was used in the current study.

All these values including conversion factors, SSDEs, DLP, CTDI_{vol}, patient age and sex were extracted and calculated by the prepared Python code.

Cancer risk assessment

To estimate the risk of breast cancer in females and lung cancer in both males and females, different models were used here which had been introduced in the BEIR VII report (NRC 2006). The following models in BEIR VII were used in the present study:

(1) The Excessive Relative Risk (ERR) model represents the excess risk relative to the background risk; (2) the Excessive Absolute Risk (EAR) model represents the absolute excess of cancer risk incidence in the study participants due to radiation exposure minus the background risk of cancer incidence in the participants; and (3) the Lifetime Attributable Risk (LAR) represents the probability of cancer induction in an individual exposed by radiation.

These models from the BEIR VII report provide different perspectives on the estimation of cancer risks associated with radiation exposure. The ERR model expresses the additional risk relative to background levels, the EAR model quantifies the excess risk in absolute terms, and the LAR model focuses on individual lifetime probability of cancer induction.

Although the ERR and EAR models are similar, the parameters in calculation and interpretation of values are different and dedicated for each model (Eq. 6).

$$\text{ERR or EAR} = \beta_s.D.\exp(\gamma e^*).\left(\frac{a}{60}\right)^{\eta}, \quad (6)$$

where β_s for the ERR model is the ERR/Sv for a 60-year-old person (attained age), who was exposed by radiation at ages $\geq$+30, while β_s for EAR model is the EAR per 10^4

Table 1 Cancer risk constants that are used in ERR and EAR models for breast and lung organs according to BEIR VII(NRC 2006)

Organ	ERR model parameters				EAR model parameters			
	B		γ	η	β		γ	η
	Male	Female			Male	Female		
Breast	–	0.51	0.00	−0.2	–	9.9[a]	−0.51	3.5, 1.1[b]
Lung	0.32	1.40	0.30	−1.4	2.3	3.4	−0.41	5.2

[a]Unlike other EAR (β_f) shown in this table, the estimate of 9.9 is for exposure at age 25 and attained age 50

[b]The first number is for attained age <50 and the second one is for attained age >50

Table 2 Demographic information of the individuals identified in the present study at the considered hospitals

Hospital #	Sex	Number of patients	Average age (year)	Max–min	SD (year)	$CTDI_{vol}$ (mGy)	DLP (mGy-cm)
Hospital 1	Male	31	47.19	14–89	17.23	17.56	615.78 ± 231.42
	Female	38	50.86	20–84	17.48	17.56	511.40 ± 228.98
Hospital 2	Male	88	45.40	4–88	18.18	6.81	248.50 ± 21.31
	Female	110	46.32	11–92	17.63	6.81	224.91 ± 36.16
Hospital 3	Male	145	47.52	12–89	17.54	5.47	176.31 ± 16.55
	Female	156	48.82	13–96	19.27	5.47	163.21 ± 17.66
Average			47.52	11.48–91.01	18.11	7.40	239.71 ± 86.16

SD standard deviation, $CTDI_{vol}$ volumetric CT dose index, *DLP* dose length product

person-years (PY)-Sv for exposure at ages above 30 and attained age 60; D is the organ dose in terms of Sv which was considered as the wSSDE in the present study; γ and η quantify the dependence of ERR and EAR on age at exposure (e) and attained age (a), respectively. Furthermore, $e*$ is defined as $(e − 30)/10$ and will be considered as zero when e is equal to 30 or higher values.

It is worth mentioning that the attained ages of 5 years plus exposure age, 10 years plus exposure age, 15 years plus exposure age, 20 years plus exposure age, 25 years plus exposure age, and 30 years plus exposure age were considered during secondary cancer risk assessment for each patient. The ERR will be expressed per Sv, while the EAR will be in per 10^4 PY-Sv. Table 1 represents the cancer risk coefficients considered for breast and lung in the current study according to the BEIR VII models.

To calculate LAR values, a "linear-no-threshold" (LNT) behavior of radiation-related cancer induction with dose was assumed, and the LAR values provided for 100 mSv ($LAR_{0.1}$) in Table 12D-2 of the BEIR-VII report were used (NRC 2006). The following equation (Eq. 7) was used to calculate the LAR, as reported per 10^5 cases exposed to a radiation dose of 0.1 Gy.

$$LAR = LAR_{0.1} \frac{SSDE}{0.1}. \tag{7}$$

Table 3 Scanning parameters that were applied in each hospital

	kV	mA	Pitch	Current modulation
Hospital 1	120	180	1.3	No
Hospital 2	130	110	1.2	Yes
Hospital 3	110	100	1.4	No

Results

This study included CT images from 570 patients who were suspected of COVID-19 infection and referred for CT scanning. The demographic information of the study participants is presented in Table 2.

To demonstrate the effect of scanning protocols on dosimetric parameters and consequently on cancer risk estimation, scanning protocol details for each specific hospital which was included in the study are provided in Table 3.

As mentioned, the estimation of cancer risk based on SSDE involved the initial step of calculating the effective diameter. The results and distribution of WED and GD for both sexes are depicted in Fig. 2.

What stands out in Fig. 2 is the disparity between GD and WED for both females and males. It is apparent that the WED value is 18% lower than the GD value in the
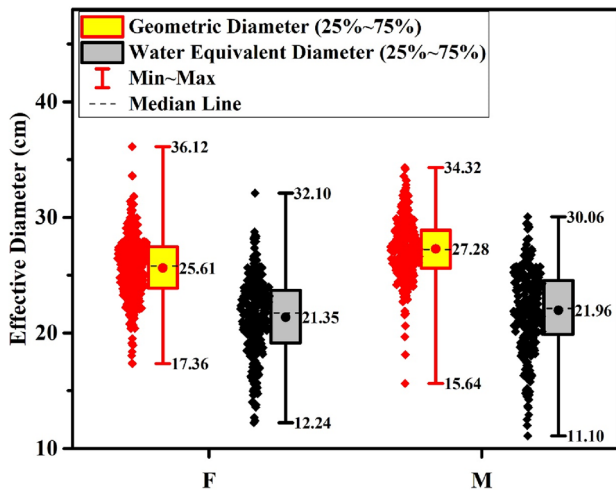
Fig. 2 Water equivalent diameter (WED) and geometric diameter (GD) values for females and males. *Filled circle* shows the mean values

studied population, and statistical analysis (*t* test) indicated that this difference is significant (*P* value < 0.001). Specifically, the mean value of the WED, regardless of gender, was equal to 21.65 cm, while the mean value of the GD was 26.45 cm. Furthermore, both the mean WED (2.78%) and GD (6.09%) values were significantly lower in females compared to males (*P* values < 0.001).

The results of the SSDE calculations based on WED and GD are presented in Fig. 3. As depicted in this figure, the mean SSDE value calculated based on WED (13.17 mGy) was higher than that calculated based on GD (10.64 mGy), and this difference was again found to be statistically significant (*P* value < 0.001) according to Kruskal–Wallis ANOVA test. The second part of Fig. 3 compares different SSDE values which were calculated based on WED in

females and males. As displayed, the mean value of SSDE for females (13.26 mGy) was slightly higher than that for males (13.08 mGy). However, in this case the statistical analysis conducted using the Kruskal–Wallis ANOVA test suggested no significant difference between these values (*P* value = 0.41).

The second dose indicator considered in this study was the effective dose. As explained previously, the effective dose was calculated based on conversion factors introduced in the AAPM TG-96 report (McCollough et al. 2008) for each specific anatomical region. Therefore, by applying a value of 0.014 mSv mGy^{-1} cm^{-1} for the thorax region, the DLP value was converted to effective dose for each patient. As a result, the mean value of the effective dose was about 3.34 mSv. Figure 4 shows the effective dose values compared in females and males. Statistical analysis based on Kruskal–Wallis ANOVA test showed a significant difference (*P* value < 0.001) between effective dose values in males and females, with a higher value in males than in females.

The estimated cancer risk in the lung and breast was calculated based on the obtained wSSDE values and BEIR VII models. Figures 5 and 6 show the ERR and EAR values for breast and lung cancer among the study participants.

Based on the Kruskal–Wallis ANOVA test there was no statistically significant difference in the calculated EAR values for lung cancer between males and females at attained age of 5 years plus exposure age and 30 years plus exposure age (*P* values 0.47 and 0.46, respectively). Similarly, there was no significant difference in the ERR values related to lung cancer between males and females at attained age of 5 years plus exposure age and 30 years plus exposure age (*P* values 0.49 and 0.45, respectively). Although there were no significant differences between EAR values for males and females at attained ages of 5 years plus exposure age and 30 years plus exposure age, reported EAR values for lung
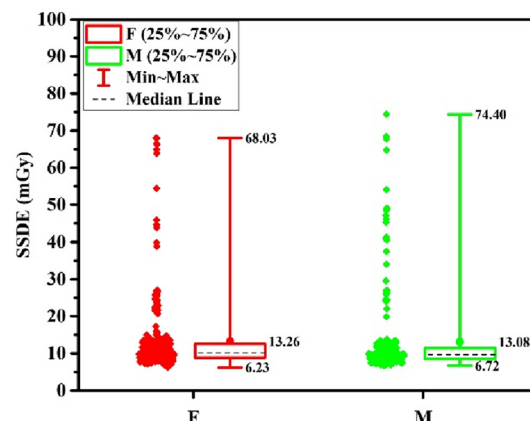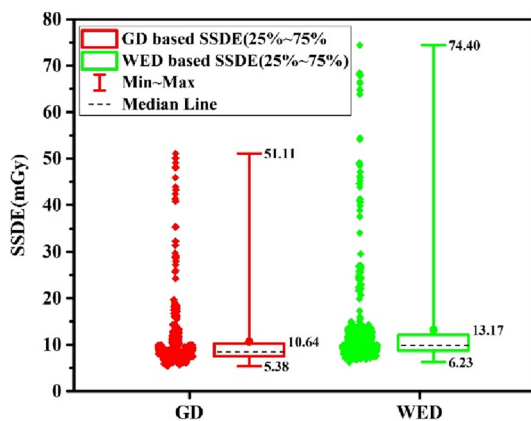

Fig. 3 Size-specific dose estimate (SSDE) values calculated based on water equivalent diameter (WED) and geometric diameter (GD). The right side of figure shows SSDE values in males and females, which

were calculated based on WED values. *Filled circle* shows mean values. *F* females, *M* males
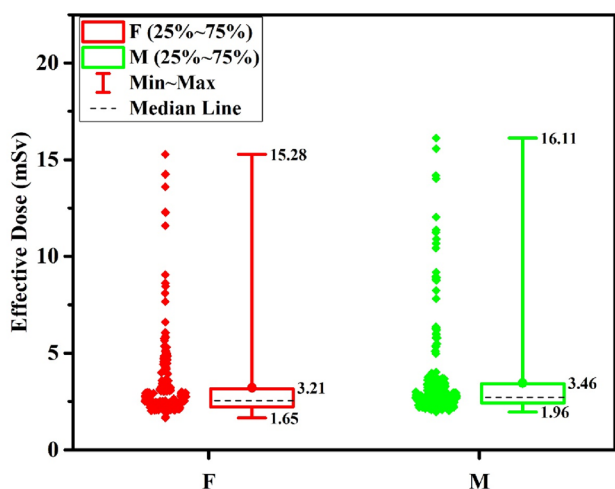
Fig. 4 Effective dose values in chest computed tomography (CT) scans between males and females in the study population. *F* females, *M* males

cancer in Fig. 5 increase with increasing the attained age. Conversely, relevant ERR values decrease with increasing the attained age. Figure 6 also supports this behavior of ERR and EAR by increasing the attained age for breast cancer.

The lung LAR was calculated for each gender based on wSSDE, and relevant descriptive values are presented in Fig. 7A. The corresponding breast cancer LAR was calculated solely for females and is illustrated in Fig. 7B.

Although the mean lung cancer LAR value was higher for females than that for males, the statistical analysis indicated no significant difference between these values (*P* value = 0.48). To assess the impact of age at exposure on the estimated LAR values, the mean value of the LAR for breast and lung cancers are reported in Table 4 in the categorized ages.

The results reveal a reduction in the LAR values for both lung and breast cancers with an increase in age at exposure.
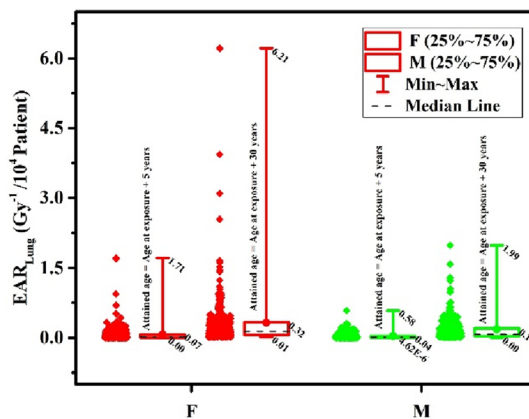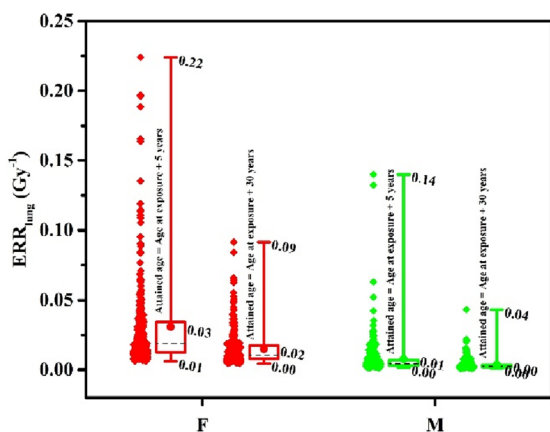

Fig. 5 Estimated excess relative risk (ERR) and excess absolute risk (EAR) values for lung based on water equivalent effective diameter (wSSDE) for males (M) and females (F). ERR and EAR values are for attained age of 5 and 30 years after age at exposure
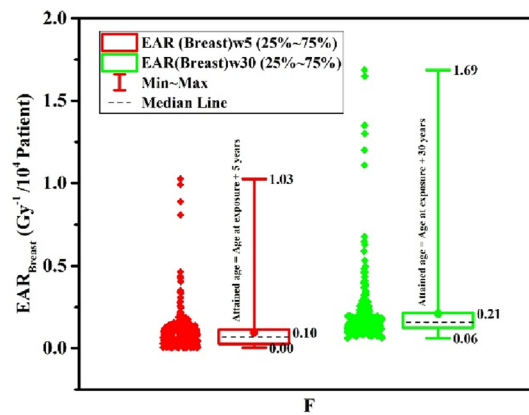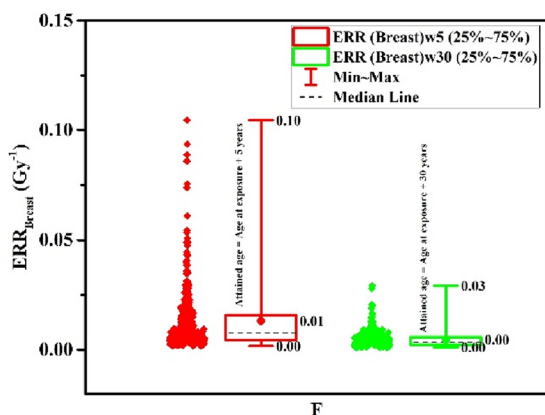

Fig. 6 Estimated excess relative risk (ERR) and excess absolute risk (EAR) values for breast cancer in females (F) based on water equivalent effective diameter (wSSDE). ERR and EAR values are for attained age of 5 and 30 years after age at exposure
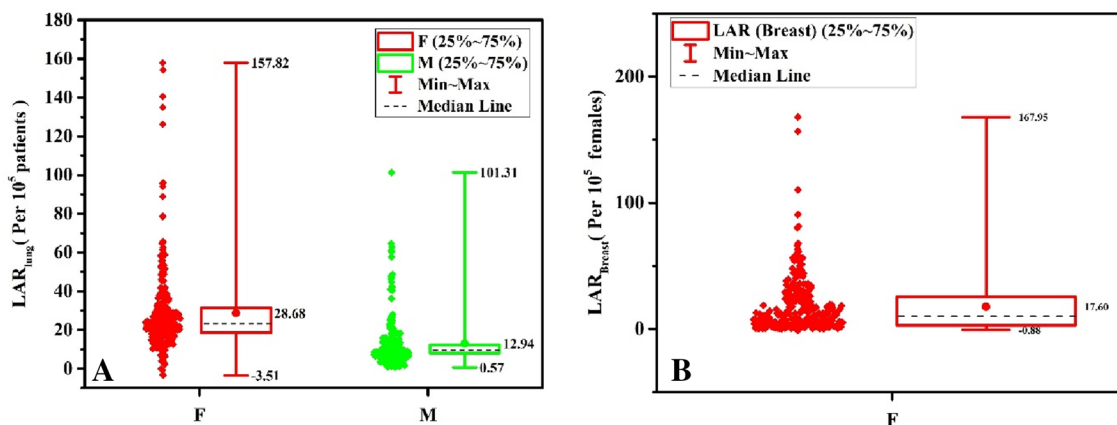
Fig. 7 **A**. Lung cancer lifetime attributable risk (LAR) values for males (M) and females (F). **B**. Breast cancer LAR values for females

Table 4 Estimated lifetime attributable risk (LAR) for breast and lung cancer in the categorized ages

Age	Number of patients in age groups	Breast cancer LAR	SE	Lung cancer LAR	SE
<20	38	33.00	5.35	37.43	3.21
21–30	61	25.00	4.07	27.93	3.09
31–40	128	10.16	1.23	19.70	1.27
41–50	107	7.66	1.04	23.87	2.35
51–60	84	3.37	0.44	21.40	1.70
61–70	86	1.65	0.18	18.17	1.54
71<	64	0.39	0.11	8.89	1.50

SE standard error

Discussion

Various studies have reported on the use of CT scans for detecting COVID-19 pneumonia (Hoda and Arash 2020; Homayounieh et al. 2020; IAEA 2020). However, there has been a concern regarding the involved radiation dose in the patients and the associated risk of radiation-related cancer. To evaluate the potential risk of radiation-related cancer associated with CT examinations, it is crucial to accurately estimate relevant organ doses. However, the evaluation of organ dose in CT scans has been a challenging issue for some time. Some studies have attempted to assess the correlation between SSDE values and organ doses in CT scans (Khatonabadi et al. 2013) Moore et al. concluded that there was a correlation better than ±10% between the SSDE values and organ doses (Moore et al. 2014). Franck et al. also studied this correlation and found a correlation of more than 80% (Franck et al. 2016). The point for the correlation of SSDE values and organ doses was the investigated organ was entirely within the scan volume.

Turner et al. studied the partial irradiation of organs in CT scans and found only a poor correlation between patient body size and organ dose (Turner et al. 2011). Gabusi et al. evaluated the effect of using water-equivalent diameters in SSDE calculations of chest CT scans (Gabusi et al. 2016). The results of their study demonstrated higher SSDE values (about 12% on average) for WED than those for GD. Based on the conclusions of the above-mentioned studies and the AAPM reports 204 and 220, WED was used in the present study to calculate patient-specific SSDE values which were then interpreted lung and breast doses. In the present study, a comparison of the GD and WED in Fig. 2 revealed that the WED value was 18% lower than the GD value. Consequently, this led to an underestimation of the calculated SSDE based on GD. The results presented in Fig. 3 further confirmed this observation by demonstrating an increase in the calculated SSDE values based on WED compared to GD. Furthermore, difference in WED values between females and males resulted in differences in SSDE values, although this difference was not statistically significant. It is worth noting that pathological opacities can affect the WED values and, consequently, changes in SSDE would be expected. Mohammadbeigi et al. conducted a study to assess the impact of pathological opacities on changes in WED and dosimetric parameters. Their findings revealed that an increase in the total severity score among COVID-19 patients resulted in higher values of SSDE when the scans were performed using automated exposure control (Mohammadbeigi et al. 2023).

Some studies reported lung and breast doses following chest CT scans to estimate the cancer risk in patients. Adeleye and Chetty (2017) reported lung doses for three different patient groups between 18.6 and 22.1 mSv. The reported dose values for breast were between 19.5 and 25.9 mSv, which were calculated using the CT-Expo software. Saltybaeva et al. reported lung doses during low-dose CT scans

following lung cancer screening using Monte Carlo calculations (Saltybaeva et al. 2016). The resulting mean lung doses were 7.7 and 0.3 mGy for standard and low-dose CT scans, respectively. In contrast, in the present report SSDE values were considered for both lung and breast dose. Based on the results shown in Fig. 3, the mean SSDE value was approximately 13.17 mGy, which aligns with the values reported in the aforementioned studies.

The second dose indicator following chest CT scans considered in the present study was the effective dose. Effective dose has been recommended for comparing the relative risk in patients undergoing CT scans relative to other imaging modalities involving ionizing radiation, especially chest radiography (Andreoli et al. 2015). The commonly used dose indicators in CT scan systems have been $CTDI_{vol}$ and DLP. It is important to note that these metrics are specific to CT scans and are not directly comparable to dose metrics used in other imaging modalities using ionizing radiation. Each imaging modality has its own specific dose metrics that is appropriate for evaluating and comparing radiation doses within that particular modality. Therefore, application of a similar dose indicator, such as the effective dose, is necessary to compare the relative risk of ionizing radiation across different imaging modalities. The effective dose takes into account the radiation doses received by various organs and tissues, considering their specific radiation sensitivities. Using the effective dose, it becomes possible to assess and compare the potential risks associated with radiation exposure from different imaging modalities. There are different approaches to estimate the effective dose in CT scans (Brady et al. 2015; Paul et al. 2012). In the present study, the conversion factor multiplied with the DLP value that was recommended by the TG 96 AAPM report was used. In the present study, the mean value of the effective dose among the study participants was approximately 3.32 mSv. This finding is consistent with the results reported in other similar studies, indicating that the radiation exposure levels in the present study align with those observed in comparable research. (Brady et al. 2015; Paul et al. 2012; Ghetti et al. 2020). Comparison of effective dose values for females and males in Fig. 4 indicates that the mean value of the effective dose in males (3.46 mSv) was slightly higher than that in females (3.21 mSv), and this difference was statistically significant. This difference can be related to differences in physical body size of males and females, which can lead to the increase in scan length and $CTDI_{vol}$. Changes in both scan length and $CTDI_{vol}$ directly can affect the effective dose.

The mean values of $CTDI_{vol}$ and DLP reported in Table 3 indicate significantly lower values compared to the values reported by Asadinezhad et al. who studied the DRL for CT examinations in Iran prior to the COVID-19 pandemic. In their study, the mean values of DLP and $CTDI_{vol}$ in the body

were 324.42 mGy cm and 8.25 mGy, respectively, whereas in the present study values of 239.71 and 7.41 mGy were observed, respectively (Asadinezhad et al. 2019).

Due to the increased demand for CT scans during the COVID-19 pandemic, special attention was given to radiation dose optimization by adjusting scanning protocols to adhere to the ALARA principle. This resulted in reductions in $CTDI_{vol}$ and DLP. However, it is important to note that the increased utilization of CT examinations during the pandemic may have led to an overall increase in the collective effective dose for patients exposed to radiation. Collective effective dose refers to the sum of individual effective doses received by a population over a specific time period. It is a measure used in radiation protection to quantify the total radiation exposure and its potential health effects on a population (Bly et al. 2015).

Another major goal of the present study was evaluating the cancer risk induction associated with the radiation dose from chest CT scans for COVID-19 patients. Three models of the BEIR-VII were used for this purpose (NRC 2006). The ERR and EAR models are suitable for determining the cancer risk induction for various cancer types, sex, age at exposure, and time after exposure to the radiation (Edward and Michael 2014). In fact, using these models, average future cancer induction risk for the population can be estimated. Figures 5 and 6 show ERR and EAR values for the induction of lung and breast cancer among study participants at attained ages of 5 and 30 years after exposure. In line with the findings of the BEIR-VII models depicted in Fig. 12-1A of this report, the present results also demonstrate a decrease in ERR values with an increase in attained age. Conversely, the EAR increases by increasing attained age. This pattern suggests that the relative risk of developing cancer decreases with age, while the absolute risk of developing cancer increases with age. The reason behind the decrease in ERR with increasing attained age is that the background cancer risk increases stronger with attained age than the EAR. Thus the ratio of both (which is the excess relative risk) decreases.

As depicted in Fig. 6, the ERR and EAR values for lung cancer were higher for females than males. This difference is largely reflected in the β factor in the BEIR VII models, which is considerably higher for females than males. Additionally, the obtained wSSDE value, which can be considered as organ dose (Fig. 3) can also be attributed to the differences in the ERR and EAR values for lungs between males and females. Although wSSDE was not significantly different between females and males, it was slightly higher in females than males.

The LAR for lung cancer, as depicted in Fig. 7, was approximately 2.21 times higher for females compared to males. As described previously, the LAR values (which were calculated for 0.1 Gy) are based on the LNT assumption on

radiation-related biological effects and the LAR values in Table 12-5A of the BEIR-VII report (NRC 2006). The risk assessment process involves addressing important factors such as variations in baseline cancer risk and the populations under study. To account for these considerations, two approaches, namely relative and absolute risk transport have been utilized. In the relative risk transport approach, the risks associated with radiation exposure are proportional to the baseline risks. On the other hand, the absolute risk transport approach assumes that radiation risks are independent of the baseline risk and are evaluated on an absolute scale. The reported values in Table 12-5A of the BEIR-VII can be calculated by both relative and absolute risk transport values. As it is evident in this table, the risk transport value of the lung were considerably higher for females than males. On the other hand, the wSSDE values calculated in our study were higher for females than for males; this could have led to higher lung LAR values for females than for males. Ghetti et al. reported that the lung LAR value was about 1.9–2.5 times higher for females than males, which is consistent with the present results. The breast LAR values for females (Fig. 7) were lower than those reported by Ghetti et al. (2020). The categorized LAR values for breast and lung cancer shown in Table 4 decrease with increasing exposure age, as expected.

Considering the anxiety patients often encounter when receiving radiation doses from CT examinations for COVID-19 screening or other application of CT scan, the findings of the present study can be useful for medical staff for considering the balancing of the image quality of CT scans against patient exposure to ionizing radiation.

Conclusion

The radiation doses received following CT scans and the corresponding potential health effects such as cancer often represent a serious concern for members of the public and for medical staff, particularly during the COVID-19 pandemic where fast screening of the possibility of an infection was required. During the pandemic, breast and lung cancer incidence possibly associated with radiation exposures due to chest CT scans received considerable attention. Following previous studies, wSSDE was used here to provide an organ dose indicator for lung and breast dose. The results of the present study showed that the doses received by these organs were not considerable. Doses received by females were slightly higher than those received by males and applying these doses in the BEIR models showed that the lung cancer incidence can be higher in females than males.

The results of the present study suggest that the cancer risks associated with CT scan exposures are not significant. Therefore, medical staff and patients should take the benefits of CT imaging for detecting such infections. It is emphasized, however, that imaging medical physicists and CT scan experts should continue to optimize the imaging protocols and balance the image quality for detecting abnormalities versus the radiation dose based on ALARA principle.

Author contributions Mostafa Robatjazi: Conceptualization, Methodology, Formal analysis, Resource, Writing - Review & Editing, Supervision, Project administration Mahdis Moayed: Methodology, Software, Validation, Investigation, Data Curation Hamid Reza Baghnai: Conceptualization, Methodology, Resource, Writing - Original Draft, Writing - Review & Editing, Supervision Mikaeil Molazadeh: Writing - Review & Editing, Data Curation, Software, Validation Nematullah Shamoossi: Resource, Writing - Review & Editing

Declarations

Conflict of interests The authors declare no competing interests.

References

Adeleye B, Chetty N (2017) Radiation dose and cancer risk estimates in helical CT for pulmonary tuberculosis infections. Open Physics 15:769–776. https://doi.org/10.1515/phys-2017-0090

Andersson J, Pavlicek W, Al-Senan R, Bolch W, Bosmans H, Cody D, Dixon R, Colombo P, Dong F, Edyvean S (2019) Estimating patient organ dose with computed tomography: a review of present methodology and required DICOM information: a joint report of AAPM task group 246 and the European Federation of Organizations for Medical Physics (EFOMP).

Andreoli S, Moretti R, Lorini FL, Lagrotta M (2015) Radiation exposure of an anaesthesiologist in catheterisation and electrophysiological cardiac procedures. Radiat Prot Dosimetry 168:76–82. https://doi.org/10.1093/rpd/ncv009

Asadinezhad M, Bahreyni Toossi MT, Nouri M (2019) Diagnostic reference levels for computed tomography examinations in Iran: a nationwide radiation dose survey. Iranian Journal of Medical Physics 16:19–26. https://doi.org/10.22038/ijmp.2018.33100.1402

Bly R, Jahnen A, Järvinen H, Olerud H, Vassileva J, Vogiatzi S (2015) Collective effective dose in Europe from X-ray and nuclear medicine procedures. Radiat Prot Dosimetry 165:129–132. https://doi.org/10.1093/rpd/ncv094

Boone JM, Strauss KJ, Cody DD, McCollough CH, McNitt-Gray MF, Toth TL, Goske MJ, Frush DP (2011) Size-specific dose estimates (SSDE) in pediatric and adult body ct examinations (trans: Subcommittee CT). https://doi.org/10.37206/143

Brady SL, Mirro AE, Moore BM, Kaufman RA (2015) How to appropriately calculate effective dose for CT using either size-specific dose estimates or dose-length product. Am J Roentgenol 204:953–958. https://doi.org/10.2214/AJR.14.13317

Edward JC, Michael KOC (2014) Estimating risk of low radiation doses—a critical review of the BEIR VII report and its use of the linear no-threshold (LNT) hypothesis. Radiat Res 182:463–474. https://doi.org/10.1667/RR13829.1

Franck C, Vandevoorde C, Goethals I, Smeets P, Achten E, Verstraete K, Thierens H, Bacher K (2016) The role of size-specific dose estimate (SSDE) in patient-specific organ dose and cancer risk estimation in paediatric chest and abdominopelvic CT examinations. Eur Radiol 26:2646–2655. https://doi.org/10.1007/s00330-015-4091-7

Gabusi M, Riccardi L, Aliberti C, Vio S, Paiusco M (2016) Radiation dose in chest CT: assessment of size-specific dose estimates based on water-equivalent correction. Physica Med 32:393–397. https://doi.org/10.1016/j.ejmp.2015.12.008

Ghetti C, Ortenzia O, Maddalo M, Altabella L, Sverzellati N (2020) Dosimetric and radiation cancer risk evaluation of high resolution thorax CT during COVID-19 outbreak. Physica Medica: European Journal of Medical Physics 80:119–124. https://doi.org/10.1016/j.ejmp.2020.10.018

Hardy AJ, Bostani M, Kim GHJ, Cagnon CH, Zankl MA, McNitt-Gray M (2021) Evaluating size-specific dose estimate (SSDE) as an estimate of organ doses from routine CT exams derived from Monte Carlo simulations. Med Phys 48:6160–6173. https://doi.org/10.1002/mp.15128

Hoda A, Arash S (2020) The role of chest CT scan in diagnosis of COVID-19. Front Emergen Med 4

Homayounieh F, Holmberg O, Umairi RA, Aly S, Basevičius A, Costa PR, Darweesh A, Gershan V, Ilves P, Kostova-Lefterova D, Renha SK, Mohseni I, Rampado O, Rotaru N, Shirazu I, Sinitsyn V, Turk T, Van Ngoc TC, Kalra MK, Vassileva J (2020) Variations in CT utilization, protocols, and radiation doses in COVID-19 pneumonia: results from 28 countries in the IAEA study. Radiology 298:E141–E151. https://doi.org/10.1148/radiol.2020203453

IAEA (2020) COVID-19 and chest CT: protocol and dose optimization.

Kang Z, Li X, Zhou S (2020) Recommendation of low-dose CT in the detection and management of COVID-2019. Eur Radiol 30:4356–4357. https://doi.org/10.1007/s00330-020-06809-6

Khatami F, Saatchi M, Zadeh SST, Aghamir ZS, Shabestari AN, Reis LO, Aghamir SMK (2020) A meta-analysis of accuracy and sensitivity of chest CT and RT-PCR in COVID-19 diagnosis. Sci Rep 10:22402. https://doi.org/10.1038/s41598-020-80061-2

Khatonabadi M, Kim HJ, Lu P, McMillan KL, Cagnon CH, DeMarco JJ, McNitt-Gray MF (2013) The feasibility of a regional CTDIvol to estimate organ dose from tube current modulated CT exams. Med Phys 40:051903. https://doi.org/10.1118/1.4798561

Li X, Samei E, Segars WP, Sturgeon GM, Colsher JG, Toncheva G, Yoshizumi TT, Frush DP (2011) Patient-specific radiation dose and cancer risk estimation in CT: Part II. Application to Patients Medical Physics 38:408–419. https://doi.org/10.1118/1.3515864

McCollough C, Bakalyar DM, Bostani M, Brady S, Boedeker K, Boone JM, Chen-Mayer HH, Christianson OI, Leng S, Li B (2014) Use of water equivalent diameter for calculating patient size and size-specific dose estimates (SSDE) in CT: the report of AAPM task group 220. AAPM Report 2014:6

McCollough C, Cody D, Edyvean S, Geise R, Gould B, Keat N (2008) Report No. 096-the measurement, reporting, and management of radiation dose in CT (2008). AAPM

Menke J (2005) Comparison of different body size parameters for individual dose adaptation in body CT of adults. Radiology 236:565–571. https://doi.org/10.1148/radiol.2362041327

Mohammadbeigi A, Shouraki JK, Ebrahiminik H, Nouri M, Bagheri H, Moradi H, Azizi A, Fadaee N, Soltanzadeh T, Moghimi Y (2023) Pathology-based radiation dose in computed tomography: investigation of the effect of lung lesions on water-equivalent diameter, CTDIVol and SSDE in COVID-19 patients. Radiat Prot Dosimetry. https://doi.org/10.1093/rpd/ncad245

Moore BM, Brady SL, Mirro AE, Kaufman RA (2014) Size-specific dose estimate (SSDE) provides a simple method to calculate organ dose for pediatric CT examinations. Med Phys 41:071917. https://doi.org/10.1118/1.4884227

NRC (2006) Health risks from exposure to low levels of ionizing radiation: BEIR VII phase 2.

Paul J, Banckwitz R, Krauss B, Vogl TJ, Maentele W, Bauer RW (2012) Estimation and comparison of effective dose (E) in standard chest CT by organ dose measurements and dose-length-product methods and assessment of the influence of CT tube potential (energy dependency) on effective dose in a dual-source CT. Eur J Radiol 81:e507–e512. https://doi.org/10.1016/j.ejrad.2011.06.006

Ravenel JG, Scalzetti EM, Huda W, Garrisi W (2001) Radiation exposure and image quality in chest CT examinations. Am J Roentgenol 177:279–284. https://doi.org/10.2214/ajr.177.2.1770279

Report 87 (2012). J ICRU 12:55–66. https://doi.org/10.1093/jicru_ndt006

Saltybaeva N, Martini K, Frauenfelder T, Alkadhi H (2016) Organ dose and attributable cancer risk in lung cancer screening with low-dose computed tomography. PLoS ONE 11:e0155722. https://doi.org/10.1371/journal.pone.0155722

Toth T, Ge Z, Daly MP (2007) The influence of patient centering on CT dose and image noise. Med Phys 34:3093–3101. https://doi.org/10.1118/1.2748113

Turner AC, Zhang D, Khatonabadi M, Zankl M, DeMarco JJ, Cagnon CH, Cody DD, Stevens DM, McCollough CH, McNitt-Gray MF (2011) The feasibility of patient size-corrected, scanner-independent organ dose estimates for abdominal CT exams. Med Phys 38:820–829. https://doi.org/10.1118/1.3533897

Vahdat P, Milad Z, Saber S, Seyed Mohammad J (2020) Clinical Performance of RT-PCR and chest CT scan for covid-19 diagnosis; a systematic review. Front Emergen Med 4

Williams TC, Wastnedge E, McAllister G, Bhatia R, Cuschieri K, Kefala K, Hamilton F, Johannessen I, Laurenson IF, Shepherd J, Stewart A, Waters D, Wise H, Templeton KE (2020) Sensitivity of RT-PCR testing of upper respiratory tract samples for SARS-CoV-2 in hospitalised patients: a retrospective cohort study. Wellcome Open Research 5:254. https://doi.org/10.12688/wellcomeopenres.16342.2